



Donor–Acceptor Type Thioxanthenes: Synthesis, Optical Properties, and Two-Photon Induced Polymerization

Rashid Nazir,[†] Evaldas Balčiūnas,[‡] Dorota Buczyńska,[§] Florent Bourquard,[‡] Dorota Kowalska,[§] David Gray,[‡] Sebastian Maćkowski,^{*,§} Maria Farsari,^{*,‡} and Daniel T. Gryko^{*,†,||}

[†]Faculty of Chemistry, Warsaw University of Technology, Noakowskiego 3, 00-664 Warsaw, Poland

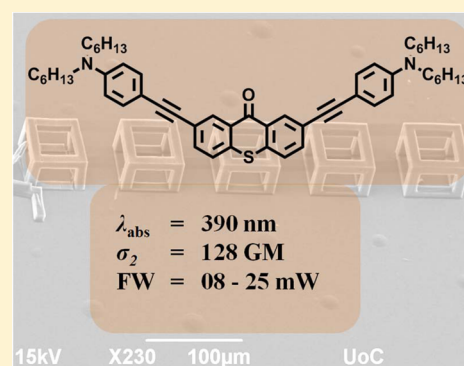
[‡]Institute of Electronic Structure and Laser (IESL), Foundation for Research and Technology Hellas (FORTH), N. Plastira 100, 70013, Heraklion, Crete Greece

[§]Department of Physics, Astronomy and Informatics, Nicolaus Copernicus University, Grudziadzka 5, 87-100 Torun, Poland

^{||}Institute of Organic Chemistry, Polish Academy of Sciences, Kasprzaka 44/52, Warsaw, Poland

Supporting Information

ABSTRACT: A set of thioxanthone derivatives bearing strongly electron-donating dialkylamino groups have been synthesized efficiently via the Buchwald–Hartwig, Sonogashira, and Heck reactions. Compounds possessing both one and two donors have been prepared. Their optical properties proved to be intriguing. The presence of the amino group alone increased the fluorescence quantum yield 100 times. Dyes possessing arylethylene and arylethynyl linkages absorbed UV radiation and violet light while emitting (weakly) red light, as a consequence of different geometries at ground and excited states. Our design led to an increase in two-photon absorption cross sections at the wavelength of interest (800 nm) to the highest values ever recorded for thioxanthenes, while maintaining excellent solubility due to the fact that all new photoinitiators are highly viscous oils at room temperature. Some of the prepared D– π –A– π –D systems also proved to be initiators in two-photon polymerization.



■ INTRODUCTION

The difference between one-photon (MPP) and two-photon induced photopolymerization (TPIP) lies in how the energy for activating the initiators is provided.¹ In TPIP, the initiators are excited to triplet states by absorbing the energy from two photons, in combination. Two-photon photopolymerization was reported in 1965 by Pao and Rentzepis² as the first example of multiphoton excitation-induced photochemical reactions. Although there were some ensuing investigations reported throughout the literature,³ no focused efforts were devoted to two-photon photopolymerization until this technology was found to be a valuable tool for micro-fabrications.⁴ The first reported 3D microstructure⁵ was a 7 mm diameter and 50 mm long spiral coil with a line cross section of 1.3–2.2 mm. Current research efforts in two-photon photopolymerization have been devoted to both the synthesis of high-efficiency photoinitiators and sensitizers⁶ as well as to establishing this methodology as a nanoprocessing tool.⁷ The use of two-photon induced photopolymerization allows for the polymerization of structures with submicron features, implying diverse uses of the technology.⁸ Great efforts have been devoted to the development of both monomers⁹ and photoinitiators for MPP,¹⁰ and several reviews have been published on this topic.¹¹ Several relevant solutions have been proposed to improve the 2PA ability of chromophores while concomitantly enhancing their photoreactivity. The additional

advantage of this technique is that the two-photon photopolymerization system resembles a laser scanning microscope, which does not need vacuum conditions for operation. Even though it is a fairly new technology, demonstrated first in 1997,⁴ direct laser writing by two-photon photopolymerization has already been employed in a variety of fields such as photonics,¹² metamaterials,¹³ microfluidics,¹⁴ and scaffolds for cell growth and tissue engineering.¹⁵

Since its first synthesis in 1890,¹⁶ thioxanthone (TX) and its derivatives have been used extensively as initiators for one-photon polymerization.¹⁷ For two-photon polymerization, the two-photon absorption cross section of unsubstituted TX was too low for any practical applications.¹⁸ Malval and co-workers synthesized naphtho[2,3-*c*]thioxanthen-8-one (ANTX) and applied it to the fabrication of 3D structures.¹⁹ These authors also measured the TPA cross section, which was 30 times higher than the value observed for any commercially available unsubstituted TX^{18,19} but still below widely known two-photon active chromophores.²⁰ The accumulated knowledge related to two-photon absorption²⁰ pointed to the following preferred architectures: D–A, D–A–D, A–D–A, D– π –A– π –A, etc. We therefore attempted to study π -expanded donor–acceptor

Received: February 16, 2015

Revised: March 29, 2015

Published: April 8, 2015



systems based on the thioxanthone moiety. Since thioxanthone itself can be considered as an electron-poor core, we proposed to decorate it with additional electron-donating groups. In particular, we resolved to investigate the influence of the presence and the character of the linker between the thioxanthone core and the electron-donating dialkylamino groups.

EXPERIMENTAL SECTION

Materials and Synthesis. All reagents and solvents were purchased from commercial sources and were used as received. DMF and toluene were dried prior to use and stored under argon. The reaction progress was monitored by thin layer chromatography (TLC) with silica gel 60 F254 with detection by a UV lamp. Product purifications were done by column chromatography with Kieselgel. Occasionally, dry column vacuum chromatography (DCVC)²¹ was performed for purification of products using silica gel Type D 5F. The following compounds were synthesized following literature procedures: 2-bromo-9H-thioxanthen-9-one (**1**),²² 4-ethynyl-*N,N*-dihexylaniline (**3**),²³ and 2,7-dibromo-9H-thioxanthen-9-one (**5**).²⁴

2-(Didodecylamino)-9H-thioxanthen-9-one (2). An oven-dried screw cap test tube equipped with a stir bar was evacuated and refilled with argon (three times). Subsequently, RuPhos (11 mg, 0.025 mmol), compound **1** (145 mg, 0.5 mmol), didodecylamine (211 mg, 0.6 mmol), Cs₂CO₃ (195 mg, 0.6 mmol), and Pd(OAc)₂ (2.4 mg, 0.010 mmol) were added to the tube, followed by the addition of toluene/*t*-BuOH (1 mL/0.2 mL) by syringe under a counter flow of argon. The tube was placed in a preheated oil bath at 120 °C, and the reaction mixture was stirred vigorously for 16 h. The reaction mixture was then cooled to room temperature, diluted with ethyl acetate, washed with water, dried over Na₂SO₄, concentrated under vacuum, and purified via DCVC (silica, CH₂Cl₂/hexanes 1:5 to 1:2) to obtain product **2** as a yellow gel with 69% yield. *R*_f = 0.6 (CH₂Cl₂/hexanes 1:1). ¹H NMR (CDCl₃, 500 MHz) δ: 8.62 (d, *J* = 8 Hz, 1H), 7.83 (s, 1H), 7.56 (d, *J* = 2.8 Hz, 1H), 7.42 (t, *J* = 7.5 Hz, 2H), 7.05 (d, *J* = 3.3 Hz, 1H), 3.37 (t, *J* = 14.5 Hz, 4H), 1.61–1.57 (m, 4H), 1.33–1.27 (m, 36H), 0.88 (t, *J* = 14 Hz, 6H). ¹³C NMR (CDCl₃, 125 MHz) δ: 180.2, 147.1, 138.0, 131.6, 130.2, 129.9, 128.9, 126.9, 126.1, 125.6, 122.7, 118.4, 110.1, 51.2, 32.0, 29.8, 29.7, 29.7, 29.6, 29.6, 29.5, 27.3, 27.2, 22.8, 14.2. HRMS (ESI): *m/z* ([*M* + *H*]⁺) C₃₇H₅₇NOS: calculated 563.4161; found: 563.4146.

2-((4-(Didodecylamino)phenyl)ethynyl)-9H-thioxanthen-9-one (4). Pd(OAc)₂ (1.7 mg, 0.008 mmol), di-*tert*-butyl-(2,2-diphenyl-1-methyl-1-cyclopropyl)phosphine (cBRIDP) (7.2 mg, 0.020 mmol), polyoxyethanyl- α -tocopheryl sebacate solution (PTS) (0.33 mL, 15 wt %), Et₃N (200 μ L, 1.44 mmol), compound **1** (145 mg, 0.50 mmol), and amine **3** (213 mg, 0.75 mmol) were added to a 5 mL round-bottom flask. The reaction progress was monitored by thin-layer chromatography (TLC). After 18 h, the reaction mixture was diluted with brine and extracted with ethyl acetate (3 times). The combined organic extracts were dried over anhydrous Na₂SO₄, filtered, and concentrated by rotary evaporation. The purification was performed via silica gel chromatography (chloroform/hexanes, 1:5) to afford the desired product **4** (221 mg, 89%) as a yellow gel. *R*_f = 0.6 (chloroform:hexanes = 1:2). ¹H NMR (CDCl₃, 500 MHz) δ: 8.61 (dd, *J*₁ = 8 Hz, *J*₂ = 8 Hz, 2H), 7.79 (d, *J* = 7 Hz, 1H), 7.67–7.63 (m, 2H), 7.50–7.43 (m, 4H), 6.64 (d, *J* = 6 Hz, 2H), 3.32 (t, *J* = 15 Hz, 4H), 1.58–1.36 (m, 4H), 1.33–1.32 (m, 36H), 0.92 (t, *J* = 14 Hz, 6H). ¹³C NMR (CDCl₃, 125 MHz) δ: 179.3, 148.1, 136.9, 134.9, 134.3, 133.08, 133.02, 132.28, 132.25, 129.9, 129.16, 129.13, 126.0, 125.9, 125.5, 111.2, 108.1, 92.6, 86.1, 50.9, 31.6, 27.1, 26.7, 22.6, 14.0. HRMS (ESI): *m/z* ([*M* + *H*]⁺) C₃₃H₃₇NOS: calculated 496.2684; found: 496.2680.

***N,N*-Didodecyl-4-vinylaniline (6).** Compound **6** was prepared based on a procedure reported previously, with some modifications.²⁵ To a Schlenk flask in an argon-filled glovebox, methyltriphenylphosphonium iodide (4.04 g, 10 mmol) and THF (25 mL) were added to a 100 mL round-bottom flask. The flask was taken out of the glovebox and cooled to –78 °C in a dry ice–acetone bath. A solution

of *n*-BuLi (1.6 M solution in hexane, 6 mL) was added via syringe under nitrogen. The reaction mixture was allowed to stir at –78 °C for 1 h and then was warmed to room temperature for another 1 h. A solution of 4-(didodecylamino)benzaldehyde (4.57 g, 10 mmol) in 10 mL of THF was added dropwise. The reaction mixture was stirred at room temperature overnight. After reaction, most of the THF was evaporated and the solution was diluted with hexane. The compound was purified using a basic alumina column yielding product **6** (4.40 g, yield 96%) as a colorless oil. ¹H NMR (CDCl₃, 500 MHz) δ: 7.27 (d, *J* = 7.5 Hz, 2 H), 6.58 (d, *J* = 9 Hz, 2 H), 5.51 (d, *J* = 18 Hz, 1 H), 4.98 (d, *J* = 9 Hz, 1 H), 3.26 (t, *J* = 15.5 Hz, 4 H), 1.58 (m, 4 H), 1.30 (m, 36 H), 0.89 (t, *J* = 14 Hz, 6H). ¹³C NMR (CDCl₃, 125 MHz) δ: 148.0, 136.7, 127.4, 124.9, 111.8, 111.5, 108.6, 51.2, 32.0, 29.8, 29.7, 29.6, 29.57, 29.50, 27.4, 27.3, 22.8, 14.2. HRMS (ESI): *m/z* ([*M* + *H*]⁺) C₃₂H₅₇N: calculated 455.4491; found: 455.4487.

2,7-Bis((*E*)-4-(didodecylamino)styryl)-9H-thioxanthen-9-one (7). An oven-dried Schlenk tube was equipped with a stir bar, evacuated, and refilled with argon (three times). Subsequently, the following compounds were added under a flow of argon: **5** (184 mg, 0.5 mmol), **6** (546 mg, 1.2 mmol), Pd(OAc)₂ (7.5 mg, 0.033 mmol), tri-*o*-tolylphosphine (20.1 mg, 0.067 mmol), Et₃N (1 mL, 7.15 mmol), and finally anhydrous DMF (4 mL). The Schlenk tube was sealed and heated at 100 °C for 20 h. The reaction mixture was then poured into 200 mL of water and extracted using ethyl acetate (100 mL \times 3 times), dried over Na₂SO₄, and concentrated under vacuum. Purification via DCVC (silica, CH₂Cl₂/hexanes 1:2) afforded the product as an orange gel with 71% yield. *R*_f = 0.6 (CH₂Cl₂/hexanes 1:1). ¹H NMR (CDCl₃, 500 MHz) δ: 8.66 (d, *J* = 2 Hz, 2H), 7.75 (dd, *J*₁ = 1.5 Hz, *J*₂ = 1.5 Hz, 2H), 7.51 (d, *J* = 8.5 Hz, 2H), 7.42 (d, *J* = 9 Hz, 4H), 7.19 (d, *J* = 16.5 Hz, 2H), 6.90 (d, *J* = 16.5 Hz, 2H), 6.64 (d, *J* = 9 Hz, 2H), 3.30 (t, *J* = 15 Hz, 8H), 1.64–1.58 (m, 8H), 1.33–1.27 (m, 72H), 0.90 (t, *J* = 14 Hz, 12H). ¹³C NMR (CDCl₃, 125 MHz) δ: 182.7, 150.7, 139.5, 137.3, 132.8, 132.0, 131.9, 130.6, 129.4, 128.8, 126.6, 124.6, 114.2, 53.7, 34.5, 32.33, 32.30, 32.28, 32.25, 32.21, 32.0, 29.9, 29.8, 25.3, 16.7. HRMS (ESI): *m/z* ([*M* + *H*]⁺) C₇₇H₁₁₉N₂OS: calculated 1119.9043; found: 1119.9048.

2,7-Bis((4-(didodecylamino)phenyl)ethynyl)-9H-thioxanthen-9-one (8). Pd(OAc)₂ (1.7 mg, 0.008 mmol), di-*tert*-butyl-(2,2-diphenyl-1-methyl-1-cyclopropyl)phosphine (cBRIDP) (7.2 mg, 0.020 mmol), polyoxyethanyl- α -tocopheryl sebacate solution (PTS) (0.33 mL, 15 wt %), Et₃N (200 μ L, 1.44 mmol), compound **5** (91 mg, 0.25 mmol), and compound **3** (213 mg, 0.75 mmol) were added to a 5 mL round-bottom flask. The reaction progress was monitored by thin-layer chromatography (TLC). After 18 h, the reaction mixture was diluted with brine and extracted with ethyl acetate (3 times). The combined organic extracts were dried over anhydrous Na₂SO₄, filtered, and concentrated by rotary evaporation. Purification via silica gel chromatography (chloroform:hexanes = 1:5) afforded the desired product **8** (187 mg, 96%) as a yellow gel. *R*_f = 0.7 (chloroform:hexanes = 1:2). ¹H NMR (CDCl₃, 500 MHz) δ: 8.72 (d, *J* = 2 Hz, 2H), 7.69 (dd, *J*₁ = 2 Hz, *J*₂ = 2 Hz, 2H), 7.51 (d, *J* = 8 Hz, 2H), 7.40 (d, *J* = 8 Hz, 4H), 6.98 (d, *J* = 8 Hz, 4H), 3.29 (t, *J* = 15 Hz, 8H), 1.60–1.56 (m, 8H), 1.34–1.32 (m, 24H), 0.90 (t, *J* = 14 Hz, 12H). ¹³C NMR (CDCl₃, 125 MHz) δ: 178.9, 148.3, 135.5, 134.5, 133.1, 132.4, 129.1, 127.7, 126.1, 123.0, 111.3, 108.2, 92.8, 86.3, 51.1, 31.8, 27.3, 26.9, 22.8, 14.1. HRMS (ESI): *m/z* ([*M* + *H*]⁺) C₅₃H₆₆N₂OS: calculated 779.4954; found: 779.4965.

2,7-Bis(didodecylamino)-9H-thioxanthen-9-one (9). RuPhos (20 mg, 0.05 mmol), compound **5** (184 mg, 0.5 mmol), didodecylamine (423 mg, 1.2 mmol), Cs₂CO₃ (390 mg, 1.2 mmol), and Pd(OAc)₂ (4.8 mg, 0.02 mmol) were added to an oven-dried screw cap test tube equipped with a stir bar. The test tube was evacuated and refilled with argon (three times) and a toluene/*t*-BuOH (2 mL/0.4 mL) mixture was added by syringe under a counterflow of argon. The tube was placed in a preheated oil bath at 120 °C, and the reaction mixture was stirred vigorously for 16 h. The reaction mixture was then cooled to room temperature, diluted with ethyl acetate, washed with water, dried over Na₂SO₄, concentrated under vacuum, and purified via DCVC (silica, chloroform/hexanes, 1:5) to afford the product as an orange gel with 53% yield. *R*_f = 0.6 (chloroform/hexanes, 1:2). ¹H NMR (CDCl₃,

500 MHz) δ : 7.8 (d, J = 2.5 Hz, 2H), 7.35 (d, J = 9.5 Hz, 2H), 6.98 (dd, J_1 = 3 Hz, J_2 = 3 Hz, 2H), 3.31 (t, J = 15.5 Hz, 8H), 1.57–1.52 (m, 8H), 1.28–1.21 (m, 72H), 0.84 (t, J = 14 Hz, 12H). ^{13}C NMR (CDCl_3 , 125 MHz) δ : 180.1, 146.5, 129.6, 127.6, 126.8, 123.7, 118.2, 110.0, 51.1, 31.1, 31.0, 29.6, 29.52, 69.5, 29.3, 29.2, 27.2, 22.6, 14.0. HRMS (ESI): m/z ($[\text{M} + \text{H}]^+$) $\text{C}_{61}\text{H}_{107}\text{N}_2\text{OS}$: calculated 915.8104; found: 915.8079.

Resin Preparation. The photopolymerizable materials used for the DLW evaluation of the photoinitiators were organic–inorganic composites described earlier.^{26a} Methacryloxypropyltrimethoxysilane (MAPTMS, Sigma-Aldrich) and methacrylic acid (MAA, Sigma-Aldrich) were the organic photopolymerizable monomers, while zirconium *n*-propoxide (ZPO, 70% in propanol, Sigma-Aldrich) and the alkoxysilane groups of MAPTMS, the moieties which form the inorganic network.

First, MAPTMS was hydrolyzed using HCl solution (0.01 M) at a ratio of 1:0.75. ZPO was separately stabilized by MAA, at a 1:1 ratio. After 45 min, the hydrolyzed MAPTMS was slowly added to the ZPO–MAA mixture, and the final hydrolysis of the composite was carried out. Finally, the photoinitiator under investigation was added to each mixture. After stirring for 24 h, the materials were filtered using 0.22 μm syringe filters.

The samples were prepared by drop-casting them onto glass substrates, and the resultant films were dried in a vacuum oven at 100 $^\circ\text{C}$ for 1 h before the photopolymerization. The heating process resulted in the condensation of the hydroxy-mineral moieties and the formation of the inorganic matrix.

Photophysics. Absorption spectra were measured using a Cary 50 spectrophotometer (Varian). Solutions of the compounds were dissolved in chloroform to a concentration of between 5×10^{-5} and 2×10^{-4} mol/dm³ and placed in quartz cuvettes with an optical path of 10 mm. To determine the molar extinction coefficients, concentrations of the compounds were varied by a few orders of magnitude with respect to the stock solution.

Fluorescence spectra were measured using a Fluorolog 3 spectrofluorometer (Yobin Ivon). Solutions were placed in quartz cuvettes. Excitation wavelengths were selected to correspond to the absorption maxima for each individual compound. To determine fluorescence quantum yields, we used quinine sulfate as a reference.

Fluorescence decays were measured using a time-correlated single photon counting technique employing a SPC-150 card (Becker and Hickl). The signal was detected using a fast avalanche photodiode (id100-20, idQuantique). For excitation, we used either diode-pumped solid state lasers or an ultra-broad-band supercontinuum source (Fianium) to excite the molecules at the maximum of the absorption. The spectral range of detection was selected by band-pass optical filters. Details of the experimental setup are described elsewhere.^{26b}

TPA Cross-Section Measurements. TPA cross-section measurement was done using the Z-scan technique, and the experimental setup has been described earlier.²⁷ Z-scan measurements for compounds 2, 4, 7, 8, and 9 were carried out at dye concentrations 0.01–0.25 mol L⁻¹ at 800 nm.

Fabrication of Microstructures with DLW Setup. The experimental setup for the 3D structure fabrication by DLW has been described before.²¹ The laser used was a Ti:sapphire femto-second laser operating at 800 nm (Femtolasers Fusion), with integrated dispersive mirrors that precompensate the beam delivery and focusing optics that achieve sub-20 fs duration pulses into the sample. The average power of the laser is 400 mW, and its repetition rate is 75 MHz. The 3D structure was generated using an *x*–*y* galvanometric mirror digital scanner (Scanlabs Hurriscan II), controlled by SAMLight (SCAPS) software, adapted to accommodate a high numerical aperture focusing microscope objective lens (100 \times , N.A. = 1.4, Zeiss, Plan Apochromat). To improve focusing, the laser beam was expanded 5 \times using a telescope. Movement on the *z*-axis and large-scale movement on the *x*–*y* plane were achieved with a three-axes linear encoder stage (PI). Beam control was achieved using a mechanical shutter (Uniblitz). The beam intensity was controlled using a motorized attenuator (Altechna). The stages, the shutter, and the attenuator were computer-controlled via a National Instruments

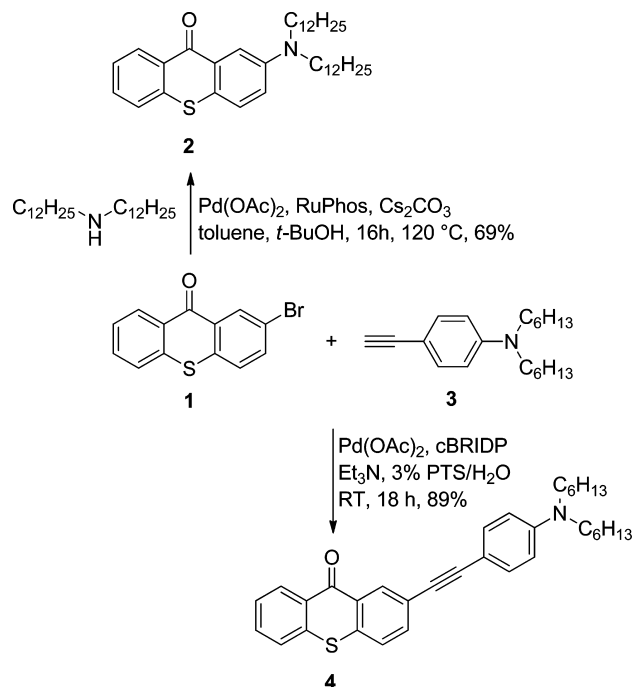
LabVIEW program. A CCD camera was mounted behind a dichroic mirror for online monitoring of the polymerization process.

The sample was mounted upside down with the glass slide facing the objective to prevent contact of the material with the oil of the objective. The structures were fabricated in a layer-by-layer fashion with the last layer positioned on the surface of the coverslip; this process prevented illumination passing through the already polymerized region. After the completion of the component building process, the sample was developed in 4-methyl-2-pentanone and rinsed in isopropanol.

RESULTS AND DISCUSSION

Bromo-substituted thioxanthenes 1 and 5 were chosen as the most convenient building blocks to build the designed donor–acceptor architectures (Schemes 1 and 2). Long alkyl chains as

Scheme 1. Synthesis of Thioxanthenes 2 and 4



solubilizing factors were employed due to the need to impart good solubility. This strategy had proven to be very efficient in previous cases. Thus, thioxanthenes 1 and 5 were reacted with didodecylamine following conditions developed by Buchwald (Scheme 1) to obtain amines 2 and 9 in yields of 69% and 57%, respectively. The π -expanded compound 7, bearing two C–C double bonds, was prepared via Heck reaction with *N,N*-didodecyl-4-vinylaniline (6) under classical conditions (Scheme 2). On the other hand, the Sonogashira reaction proved more problematic. Typical conditions^{23,29} failed to give any isolable product. Eventually, we followed the new idea recently published by Lipshutz and co-workers,³⁰ namely the cross-coupling reactions between aryl bromide and terminal alkynes in micelles, in the absence of copper. Using the reported procedure, compounds 4 and 8 were synthesized via intermediate 3 (Schemes 1 and 2).

Optical Properties. The presence of auxochromic dialkylamino groups shifted the absorption of thioxanthenes 2 and 9 bathochromically by 80–110 nm (Table 1, Figures 2 and 3). These compounds emit yellow light, and their Stokes shifts were moderate (~ 3500 cm⁻¹). On the other hand, π -expansion of the system did not lead to a significant

Scheme 2. Synthesis of Thioxanthenes 7 and 8

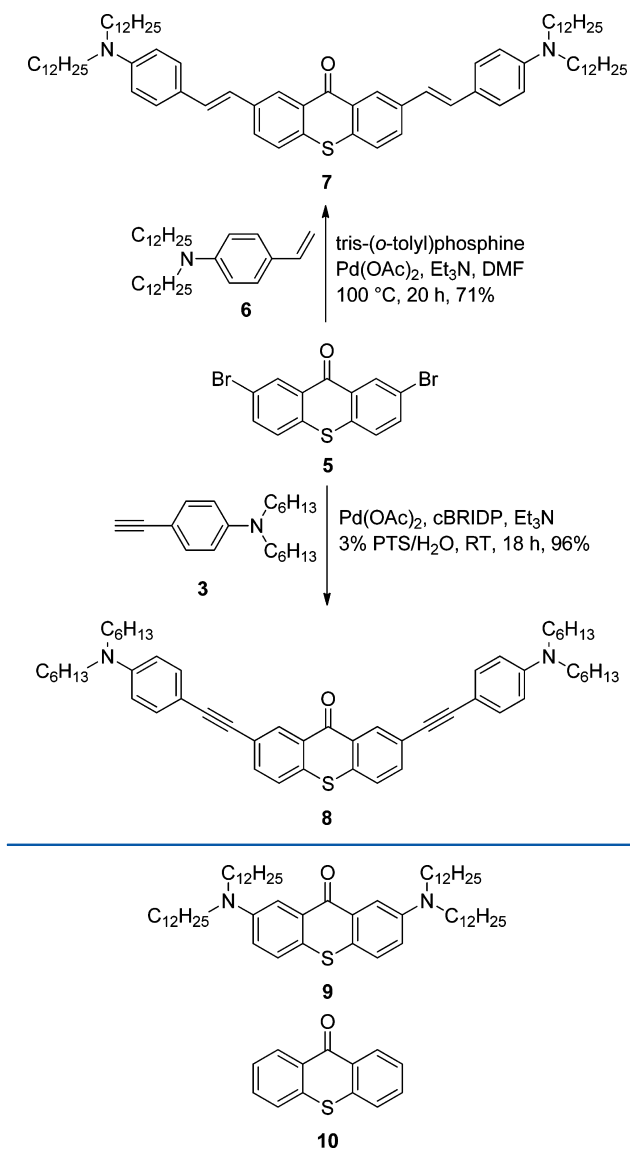


Figure 1. Structures of thioxanthenes 9 and 10.

bathochromic shift in compounds 4, 7, and 8, although the molar absorption coefficient increased by a factor of 5–10. Compounds 4, 7, and 8 were slightly yellowish, and although they emitted red light, the fluorescence quantum yield of these compounds is very low (below 0.02, determined with an accuracy better than 10%). Still, the Stokes shifts were large. The lack of a bathochromic shift for compounds 4, 7, and 8 was actually an advantage as far as two-photon absorption was concerned. These compounds were not centrosymmetric, and

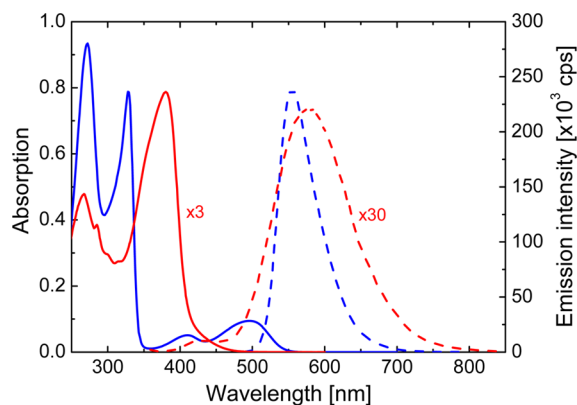


Figure 2. Absorption (solid lines) and corrected emission (dashed lines) spectra of compounds 8 (red) and 9 (blue) dissolved in chloroform. Solutions were excited at $\lambda_{\text{exc}} = 350$ nm (8) and 480 nm (9). Spectra of compound 8 were multiplied by indicated factors. The concentration of 8 is roughly 3×10^{-5} M, while the concentration of 9 is 1×10^{-4} M.

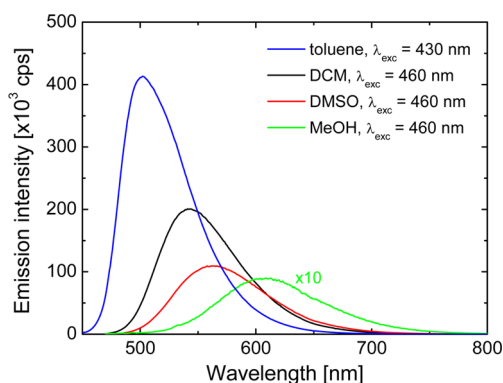


Figure 3. Fluorescence spectra of compound 2 in various solvents: toluene (blue, $c \sim 2.5 \times 10^{-5}$ M), DCM (black, $c \sim 2.5 \times 10^{-5}$ M), DMSO (red, $c \sim 1 \times 10^{-5}$ M), MeOH (green: multiplied 10 \times ; $c \sim 5 \times 10^{-5}$ M).

thus, one can expect their maxima for two-photon absorption cross section (σ_2) to be around 800 nm, which corresponds exactly to the laser wavelength typically used to achieve high spatial resolution. The weak emission of these compounds increases the chance for significant photoinitiating activity, although one has to remember that many pathways for nonradiative energy dissipation exist. As shown by Meier,³¹ the carbon–carbon double bond has stronger conductivity for D–A interactions, and our observations corroborated these data showing that compound 7 had undergone a bathochromic shift of both absorption and emission with respect to dye 8. Needless to say, thioxanthone derivatives 2 and 9 possessed the

Table 1. Spectroscopic Properties of Synthesized Dyes

compd	c [μM]	λ_{abs} [nm]	λ_{em} [nm]	Stokes shift [cm^{-1}]	ϵ_{max} [$\text{M}^{-1} \text{cm}^{-1}$]	Φ_{f}^a	τ [ns] (λ_{exc} [nm])
2	50	463	554	3500	4400	0.25	18.0 (450)
4	40	366	603	11000	22700	0.015	2.0 (405)
7	16	388	616	10000	71100	0.0044	2.9 (450)
8	~ 30	380	604	10000	~ 43700	0.015	2.0 (405)
9	50	497	560	2300	4600	0.16	14.7 (488)

^aDetermined with quinine sulfate in H_2SO_4 (0.5 M) as a standard.

highest fluorescence quantum yields recorded to date for this family of heterocycles.

The characteristic phenomenon of these compounds was their strong solvato-fluorochromism (illustrated in Figure 3 for compound 2). While absorption does not depend on the type of solvent, emission becomes bathochromically shifted and weaker as the solvent polarity increases.

Z-Scan Technique. Two-photon absorption cross sections were measured using the Z-scan method at 800 nm (Table 2).

Table 2. TPA Cross-Section Values of the Compounds 2, 4, 7, 8, and 9 Measured by Z-Scan at 800 nm

compd	solvent	concn (mol/L)	σ_2 (GM)
2	DCM	0.05	4
4	DCM	0.01	22
7	DCM	0.01	73
8	DCM	0.01	128
9	DCM	0.05	9

The values ranged from 4 to 128 GM, much higher than the reported value¹⁸ for 9H-thioxanthen-9-one (10, 3 ± 1 GM at 710 nm). The synthesized dyes 2 and 9, which possess small TPA cross sections, varied in the size of their π -conjugated system from compounds 4, 7, and 8. The maximum σ_2 value (at 800 nm) was measured for dye 8, which possesses a $C\equiv C$ bond as a linker.

Fabrication Properties. We investigated the potential for one-photon polymerization of the synthesized photoinitiators by polymerizing drop-cast films. All dyes (i.e., 2, 4, and 7–10) were dissolved in methyl methacrylate (1:1000), and the resulting mixture was exposed to UV irradiation (wide-spectrum UV lamp) for a short time. In all cases, polymerization occurred within a few minutes.

When studying the two-photon initiation potential of the synthesized materials, we took into account the following four factors: (a) The polymerization threshold: the lowest laser power required in order to fabricate structures that survived the development stage, denoted by yellow in Figure 4. In general,

these structures were deformed. (b) The good structuring threshold: the lowest laser power required to fabricate structures without deformations, denoted with green in Figure 4. (c) The burning threshold: the laser power at which microexplosions start occurring and the material starts burning. Denoted with red in Figure 4. (d) The fabrication window (FW): the power difference between the polymerization threshold and the burning threshold. A large FW is helpful, as it permits the use of higher power laser, allowing fabrication at manufacturing scales. As a reference, we used 9H-thioxanthen-9-one (10), a commercially accessible photoinitiator sometimes utilized in MPP, due to its well-established activity and its structural similarity to compounds 2, 4, and 7–9.

Compounds 2, 4, 7, 8, 9, and 10 (1%, w/w) were mixed with the hybrid composite, and the polymerization thresholds were found by fabricating microstructures at different laser powers. The results are summarized in the table of Figure 4. It was possible to fabricate structures using compounds 2, 4, 8, 9, with 2 holding the broadest FW. It was not possible to make any structures using compounds 7 and 10, as there was an overlap of the polymerization threshold with the burning threshold.

The relationship between the fabrication window, the compound's structure, and its σ_2 is far from obvious. It must be emphasized that the overall performance of a given photoinitiator depends on the product of σ_2 and the photoinitiating ability. In the case of dye 2, it is clear that although its two-photon absorption cross section is small, the quantum yield of the formation of the radicals must be high in analogy to 4,4'-(dimethylamino)benzophenone and its analogues. A similar effect, albeit to a smaller extent, can be observed for bis-amine 9. The lack of photoinitiating activity of dye 7 must be associated with the fact that the presence of two C–C double bonds triggers a different pathway of releasing the energy from the excited states. Most plausibly, E–Z isomerization takes place instead of an intersystem crossing followed by radical formation. Compound 8 has the best photoinitiating threshold, which corresponds to its relatively large two-photon absorption cross section.

Figure 5a shows an example of 2D squares fabricated employing the photopolymer with photoinitiator 2 and with decreasing laser power (left to right). Clearly, as the laser power decreases, the structures transform from burned, to well-defined, to partly written. Figure 5b shows an SEM micrograph of a hollow 3D semisphere with spikes on the surface fabricated using photoinitiator 4. The structure is deformed, indicating that it did not polymerize fully. In general, none of the thioxanthone derivatives presented here compared favorably with the standard photoinitiator we use for this photopolymer, i.e., (4,4-bis(diethylamino)benzophenone.

CONCLUSIONS

Our research has shown that simple donor–acceptor interactions are not strong enough to achieve large two-photon absorption cross sections in the thioxanthone series. Still, the combined effect of the expansion of the π -system with the presence of dialkylamino groups at the periphery generated compounds with the highest TPA cross sections achieved for thioxanthenes so far (>100 GM). We have also shown that in these π -expanded systems the interaction between electron-donating amino groups, and the heterocyclic core is different in the ground state versus the excited state, leading eventually to large Stokes shifts. Decorating thioxanthone with electron-

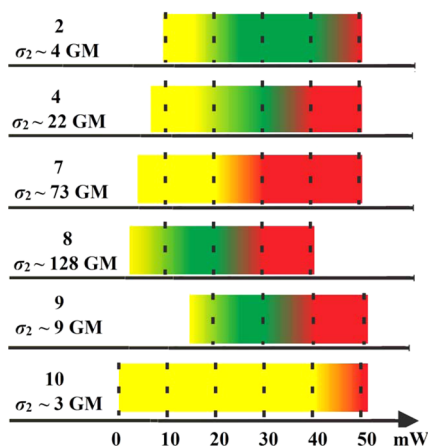


Figure 4. TPA cross sections, fabrication windows, and threshold values of compounds 2, 4, 7, 8, 9, and 10. For each compound, the threshold values are indicated by color: the polymerization threshold, yellow; the good structuring threshold, green; the burning threshold, red. The power difference between the polymerization threshold and the burning threshold defines the fabrication window for each compound.

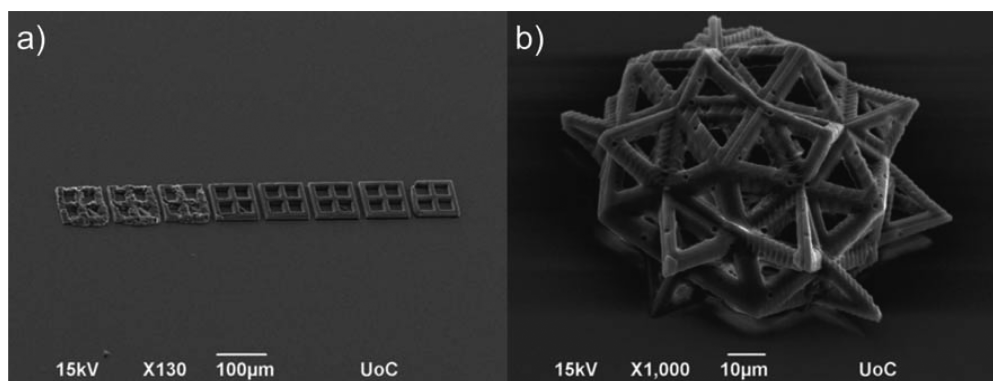


Figure 5. (a) SEM micrograph showing an array of microstructures fabricated using the photoinitiator **2** and with decreasing the average laser power. (b) SEM micrograph of a hollow 3D semisphere with spikes on the surface fabricated using photoinitiator **4**.

donating substituents and/or π -expanding the chromophore improved the performance of the prepared derivatives (versus their parent compounds) as photoinitiators in two-photon induced polymerization.

■ ASSOCIATED CONTENT

● Supporting Information

^1H NMR and ^{13}C NMR spectra of compounds **2**, **4**, **6**, **7**, **8**, and **9**, fluorescence decay curves measured for all the samples at given excitation wavelengths together with fits; fluorescence spectrum of compound **7**. This material is available free of charge via the Internet at <http://pubs.acs.org>.

■ AUTHOR INFORMATION

Corresponding Authors

*E-mail dtgryko@icho.edu.pl (D.T.G.).

*E-mail mfarsari@iesl.forth.gr (M.F.).

*E-mail mackowski@fizyka.umk.pl (S.M.).

Notes

The authors declare no competing financial interest.

■ ACKNOWLEDGMENTS

The research leading to these results has received funding from the European Community's Seventh Framework Marie Curie ITN programs TopBio (PITN-GA-2010-264362) and Angio-MatTrain (Grant Agreement 317304), from the Ministry of Science and Higher Education of the Republic of Poland (Grant MAESTRO-2012/06/A/ST5/00216), and also from the National Research and Development Center (NCBiR) under Grant ORGANOMET PBS2/AS/40/2014.

■ REFERENCES

- (1) Maruo, S.; Ikuta, K. *Appl. Phys. Lett.* **2000**, *76*, 2656–2658.
- (2) Pao, Y.-H.; Rentzepis, P. M. *Appl. Phys. Lett.* **1965**, *6*, 93–95.
- (3) (a) Chin, S. L.; Bédard, G. *Phys. Lett.* **1971**, *36A*, 271–272. (b) Papoukova, Z.; Pola, J.; Bastl, Z.; Tiaskal, J. *J. Macromol. Sci., Chem.* **1990**, *A27*, 1015. (c) Morita, H.; Sadakiyo, T. *J. Photochem. Photobiol., A* **1995**, *87*, 163.
- (4) Malinauskas, M.; Farsari, M.; Piskarskas, A.; Juodkazis, S. *Phys. Rep.* **2013**, *533*, 1–31.
- (5) Maruo, S.; Nakamura, O.; Kawata, S. *Opt. Lett.* **1997**, *22*, 132–134.
- (6) (a) Li, Z. Q.; Torgersen, J.; Ajami, A.; Muhleder, S.; Qin, X. H.; Husinsky, W.; Holnthoner, W.; Ovsianikov, A.; Stampfl, J.; Liska, R. *RSC Adv.* **2013**, *3*, 15939–15946. (b) Nazir, R.; Bourquard, F.; Balčiūnas, E.; Smoleň, S.; Gray, D.; Tkachenko, N. V.; Farsari, M.; Gryko, D. T. *ChemPhysChem* **2015**, *16*, 682–690. (c) von Freymann,

- G.; Ledermann, A.; Thiel, M.; Staude, I.; Essig, S.; Busch, K.; Wegener, M. *Adv. Funct. Mater.* **2010**, *20*, 1038–1052. (d) Hao, F.; Liu, Z.; Zhang, M.; Liu, J.; Zhang, S.; Wu, J.; Zhou, H.; Tian, Y. *Spectrochim. Acta, Part A* **2014**, *118*, 538–542. (e) Li, Z.; Pucher, N.; Cicha, K.; Torgersen, J.; Ligon, S. C.; Ajami, A.; Husinsky, W.; Rosspeintner, A.; Vauthey, E.; Naumov, S.; Scherzer, T.; Stampfl, J.; Liska, R. *Macromolecules* **2013**, *46*, 352–361. (f) Pucher, N.; Rosspeintner, A.; Satzinger, V.; Schmidt, V.; Gescheidt, G.; Stampfl, J.; Liska, R. *Macromolecules* **2009**, *42*, 6519–6528. (g) Lu, W.-E.; Dong, X.-Z.; Chen, W.-Q.; Zhao, Z.-S.; Duan, X.-M. *J. Mater. Chem.* **2011**, *21*, 5650–5659. (h) Nazir, R.; Danilevicius, P.; Gray, D.; Farsari, M.; Gryko, D. T. *Macromolecules* **2013**, *46*, 7239–7244.

- (7) (a) Marino, A.; Desii, A.; Pellegrino, M.; Pellegrini, M.; Filippeschi, C.; Mazzolai, B.; Mattoli, V.; Ciofani, G. *ACS Nano* **2014**, *8*, 11869–11882. (b) Kufelt, O.; El-Tamer, A.; Sehring, C.; Wolter, S. S.; Chichkov, B. N. *Biomacromolecules* **2014**, *15*, 650–659. (c) Marco, C. M.; Gaidukeviciute, A.; Kiyan, R.; Eaton, S. M.; Levi, M.; Osellame, R.; Chichkov, B. N.; Turri, S. *Langmuir* **2013**, *29*, 426–431.

- (8) (a) Sun, H.-B.; Kawata, S. *Adv. Polym. Sci.* **2004**, *170*, 169–273. (b) Lee, K.-S.; Yang, D.-Y.; Park, S. H.; Kim, R. H. *Polym. Adv. Technol.* **2006**, *17*, 72–82. (c) Belfield, K. D.; Morales, A. R.; Kang, B.-S.; Hales, J. M.; Hagan, D. J.; Stryland, E. W. V.; Chapela, V. M.; Percino, J. *Chem. Mater.* **2004**, *16*, 4634–4641. (d) Hales, J. M.; Hagan, D. J.; Stryland, E. W. V.; Schafer, K. J.; Morales, A. R.; Belfield, K. D.; Pacher, P.; Kwon, O.; Zojer, E.; Bredas, J. L. *J. Chem. Phys.* **2004**, *121*, 3152–3160. (e) Belfield, K. D.; Schafer, K. J.; Mourad, W.; Reinhardt, B. A. *J. Org. Chem.* **2000**, *65*, 4475–4481. (f) Martineau, C.; Anémian, R.; Andraud, C. W. I.; Bouriau, M.; Baldeck, P. L. *Chem. Phys. Lett.* **2002**, *362*, 291–295. (g) He, G. S.; Tan, L.-S.; Zheng, Q.; Prasad, P. N. *Chem. Rev.* **2008**, *108*, 1245–1330.

- (9) Ciuciu, A. I.; Cywinski, P. J. *RSC Adv.* **2014**, *4*, 45504–45516.

- (10) (a) Cumpston, B. H.; Ananthavel, S. P.; Barlow, S.; Dyer, D. L.; Ehrlich, J. E.; Erskine, L. L.; Heikal, A. A.; Kuebler, S. M.; Lee, I. Y. S.; Maughon, D.-M.; Qin, J.; Rockel, H.; Rumi, M.; Wu, X.-L.; Marder, S. R.; Perry, J. W. *Nature* **1999**, *398*, 51–54. (b) Lalevee, J.; Xiao, P.; Telitel, S.; Lepeltier, M.; Dumur, F.; Savary, F. M.; Gigmès, D.; Fouassier, J. P. *Beilstein J. Org. Chem.* **2014**, *10*, 863–876.

- (11) (a) Belfield, K. D.; Schafer, K. J. *ACS Symp. Ser.* **2003**, *847*, 464–481. (b) LaFratta, C. N.; Fourkas, J. T.; Baldacchini, T.; Farrer, R. A. *Angew. Chem., Int. Ed.* **2007**, *46*, 6238–6258. (c) Belfield, K. D.; Schafer, K. J.; Liu, Y.; Liu, J.; Ren, X.; Van Stryland, E. W. *J. Phys. Org. Chem.* **2000**, *13*, 837–849. (d) Maruo, S.; Fourkas, J. T. *Laser Photonics Rev.* **2008**, *2*, 100–111.

- (12) Gansel, J. K.; Thiel, M.; Rill, M. S.; Decker, M.; Bade, K.; Saile, V.; von Freymann, G.; Linden, S.; Wegener, M. *Science* **2009**, *325*, 1513–1515.

- (13) Kenanakis, G.; Xomalis, A.; Selimis, A.; Vamvakaki, M.; Farsari, M.; Kafesaki, M.; Soukoulis, C. M.; Economou, E. N. *ACS Photonics* **2015**, *2*, 287–294.

- (14) (a) Amato, L.; Gu, Y.; Bellini, N.; Eaton, S. M.; Cerullo, G.; Osellame, R. *Lab Chip* **2012**, *12*, 1135–1142. (b) Olsen, M. H.;

Hjorto, G. M.; Hansen, M.; Met, O.; Svane, I. M.; Larsen, N. B. *Lab Chip* **2013**, *13*, 4800–4809.

(15) (a) Torgersen, J.; Ovsianikov, A.; Mironov, V.; Pucher, N.; Qin, X. H.; Li, Z. Q.; Cicha, K.; Machacek, T.; Liska, R.; Jantsch, V.; Stampfl, J. *J. Biomed. Opt.* **2012**, *17*, 105008. (b) Torgersen, J.; Qin, X. H.; Li, Z. Q.; Ovsianikov, A.; Liska, R.; Stampfl, J. *Adv. Funct. Mater.* **2013**, *23*, 4542–4554. (c) Chatzinikolaidou, M.; Rekstyte, S.; Danilevicius, P.; Pontikoglou, C.; Papadaki, H.; Farsari, M.; Vamvakaki, M. *Mater. Sci. Eng., C* **2015**, *48*, 301–309. (d) Melissinaki, V.; Gill, A. A.; Ortega, I.; Vamvakaki, M.; Ranella, A.; Haycock, J. W.; Fotakis, C.; Farsari, M.; Claeysens, F. *Biofabrication* **2011**, *3*, 045005.

(16) Ziegler, J. H. *Ber. Dtsch. Chem. Ges* **1890**, *23*, 2469–2472.

(17) (a) Balta, D. K.; Arsu, N.; Yagci, Y.; Jockusch, S.; Turro, N. J. *Macromolecules* **2007**, *40*, 4138–4141. (b) Balta, D. K.; Bagdatli, E.; Arsu, N.; Ocal, N.; Yagci, Y. *J. Photochem. Photobiol., A* **2008**, *196*, 33–37. (c) Timpe, H. J.; Kronfeld, K. P.; Lammel, U.; Fouassier, J. P.; Lougnot, D. J. *J. Photochem. Photobiol., A* **1990**, *52*, 111–122.

(18) Schafer, K. J.; Hales, J. M.; Balu, M.; Belfield, K. D.; Stryland, E. W. V.; Hagan, D. J. *J. Photochem. Photobiol., A* **2004**, *162*, 497–502.

(19) Malval, J. P.; Jin, M.; Morlet-Savary, F.; Chaumeil, H.; Defoin, A.; Soppera, O.; Scheul, T.; Bouriau, M.; Baldeck, P. L. *Chem. Mater.* **2011**, *23*, 3411–3420.

(20) (a) Pawlicki, M.; Collins, H. A.; Denning, R. G.; Anderson, H. L. *Angew. Chem., Int. Ed.* **2009**, *48*, 3244–3266. (b) Kim, H. M.; Cho, B. R. *Chem. Commun.* **2009**, 153–164. (c) He, G. S.; Tan, L.-S.; Zheng, Q.; Prasad, P. N. *Chem. Rev.* **2008**, *108*, 1245. (d) Terenziani, F.; Katan, C.; Badaeva, E.; Tretiak, S.; Blanchard-Desce, M. *Adv. Mater.* **2008**, *20*, 4641. (e) Parthenopoulos, D. A.; Renzepis, P. M. *Science* **1989**, *245*, 843. (f) Corredor, C. C.; Huang, Z.-L.; Belfield, K. D.; Morales, A. R.; Bondar, M. V. *Chem. Mater.* **2007**, *19*, 5165.

(21) Pedersen, D. S.; Rosenbohm, C. *Synthesis* **2001**, *16*, 2431–2434.

(22) Gilman, H.; Diehl, J. W. *J. Org. Chem.* **1959**, *24*, 1914–1916.

(23) Mongin, O.; Porres, L.; Moreaux, L.; Mertz, J. *Org. Lett.* **2002**, *4*, 719–722.

(24) Coleman, M. P.; Boyd, M. K. *J. Org. Chem.* **2002**, *67*, 7641–7648.

(25) Wei, P.; Bi, X. D.; Wu, Z.; Xu, Z. *Org. Lett.* **2005**, *7*, 3199–3202.

(26) (a) Ovsianikov, A.; Viertel, J.; Chichkov, B.; Oubaha, M.; MacCraith, B.; Sakellari, I.; Giakoumaki, A.; Gray, D.; Vamvakaki, M.; Farsari, M.; Fotakis, C. *ACS Nano* **2008**, *2*, 2257–2262. (b) Krajnik, B.; Schulte, T.; Piątkowski, D.; Czechowski, N.; Hofmann, E.; Mackowski, S. *Cent. Eur. J. Phys.* **2011**, *9*, 293–299.

(27) Nazir, R.; Danilevicius, P.; Ciuciu, A. I.; Chatzinikolaidou, M.; Gray, D.; Flamigni, L.; Farsari, M.; Gryko, D. T. *Chem. Mater.* **2014**, *26*, 3175–3184.

(28) Sakellari, I.; Kabouraki, E.; Gray, D.; Purlys, V.; Fotakis, C.; Pikulin, A.; Bityurin, N.; Vamvakaki, M.; Farsari, M. *ACS Nano* **2012**, *6*, 2302–2311.

(29) Sonogashira, K.; Tohda, Y.; Hagihara, N. *Tetrahedron Lett.* **1975**, *16*, 4467–4470.

(30) Lipshutz, B. H.; Chung, D. W.; Rich, B. *Org. Lett.* **2008**, *10*, 3793–3796.

(31) Meier, H. *Angew. Chem., Int. Ed.* **2005**, *44*, 2482–2506.